arXiv:nucl-ex/0510077v1 27 Oct 2005

For Publisher's use

HAS THE QUARK-GLUON PLASMA BEEN SEEN?

J. STACHEL

Physikalisches Institut, Ruprecht-Karls-Universität Heidelberg, Philosophenweg 12, D 69120 Heidelberg, Germany

E-mail: stachel@physi.uni-heidelberg.de

1 Introduction

Very shortly after the discovery of asymptotic freedom [1] it became apparent that, as a consequence, at high temperature and/or at high density quarks and gluons would also become deconfined [2], leading to a phase transition from confined hadronic matter to an unconfined phase. This was studied in subsequent years and since the early 1980ies this phase is called the Quark-Gluon Plasma (QGP).

The conditions for this phase transition were studied in lattice QCD and state of the art calculations [3] obtain as critical temperature for the phase transition for two light and one heavier quark flavors a value for the critical temperature of $T_c = 173 \pm 15$ MeV and for the critical energy density of $\epsilon_c = 0.7 \pm 0.2$ GeV/fm^3. It is believed since many years that in collisions of heavy atomic nuclei at high energies such conditions should be reached. This motivated an experimental program starting simultaneously in 1986 at the Brookhaven AGS and at the CERN SPS, initially with light projectile nuclei such as Si and S and from 1992 and 1994, respectively, with Au and Pb projectiles. The experimental results from this program prompted a press release from CERN [4] in February 2000 stating that the combined results from the experiments proved that a new state of matter other than ordinary hadronic matter had been created in these collisions, in which quarks were 'liberated to roam freely'. The experimental results were clearly not reconcilable with the known hadronic physics and it could be estimated that the critical temperature had been exceeded in the early phase of the collision by about 20-30 % and the critical energy density by somewhat more than a factor 2. On the other hand, from those data nothing could be said yet that would characterize the properties of the new state of matter. Hence, at that time the term QGP was not used for the new state of matter.

In the summer of 2000, RHIC as a dedicated collider for heavy ions started operation with two large experiments, PHENIX and STAR, and two smaller experiments, BRAHMS and PHOBOS. In the first 3 years of operation data for Au + Au collisions with an integrated luminosity of 85/μb, for p + p collisions with 2/pb, and for d + Au collisions with 25/nb were collected and a summary of the results was recently published in a special issue of Nuclear Physics A by all four heavy ion experiments [5,6,7,8]. In the 2004 Au + Au run the 1/nb level was exceeded and data start to appear from this run. Here I will rely mostly on published data and review some of the key observations from the first 3 years including only a few of the still preliminary first run4 observations.

2 Experimental Results

2.1 Hadron Production and Statistical Models

Hadron yields have been measured for a large range of species at the AGS, SPS and at RHIC. It was realized already for many years that the data for central collisions of heavy nuclei can be rather accurately reproduced by calculations for a chemically equilibrated system in terms of a grand canonical ensemble (a review and complete set of references

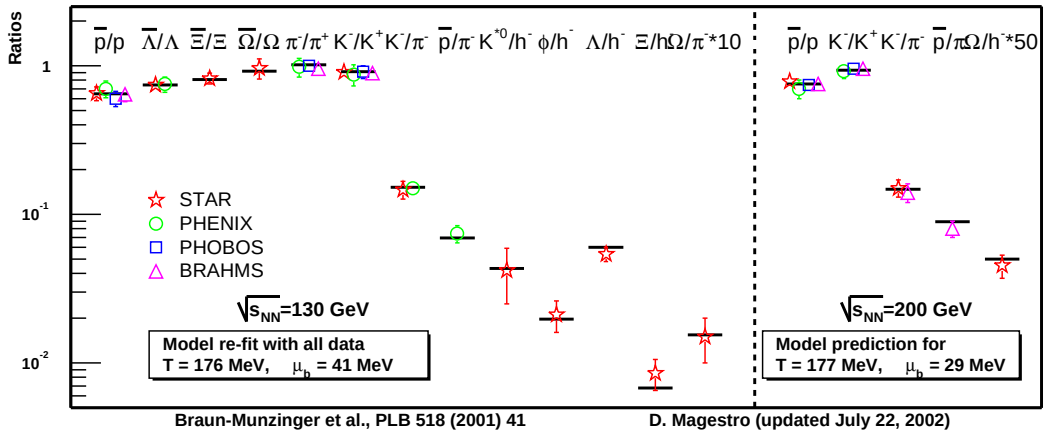

Figure 1. Hadron yield ratios measured at RHIC in comparison to calculations within a statistical model based on a grand canonical ensemble (updated version of [10], taken from [9]).

can be found in [9]). For the lower RHIC energy of $\sqrt{s} = 130$ GeV the data are final and published and for 200 GeV data are emerging currently. Figure 1 shows experimental yield ratios from all four RHIC experiments in comparison to a statistical model fit.

In the calculations, there are two free fit parameters, the temperature and the baryon chemical potential. For top RHIC energy the temperature is fitted as 177± 5 MeV, practically unchanged from $\sqrt{s} = 130$ and 17.3 GeV; the baryo-chemical potential is dropping continuously with increasing beam energy reflecting an increasing transparency of the nuclei at higher energies and an increasing dominance of baryon-antibaryon production. This is shown in Figure 2 where results of statistical model fits at various beam energies are summarized and shown together with recent results from lattice QCD [12].

It appears that from top SPS energy upwards the temperature at which hadro-chemical equilibrium is achieved is not changing anymore and practically coincides with the lattice QCD prediction for the critical temperature, while at lower beam energies it is falling. At $\sqrt{s} = 8.8$ GeV it is only 148 ± 5 MeV. The strangeness suppression that

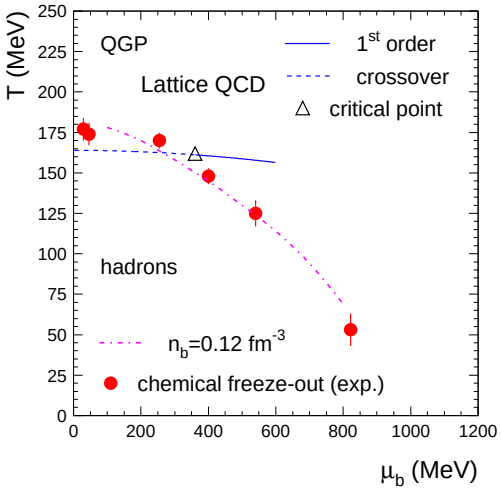

Figure 2. Phase diagram of nuclear matter in the temperature - baryon chemical potential plane. Experimental points for hadro-chemical freeze-out are shown together with a recent lattice QCD calculation [12] and a curve of constant total baryon density. Figure from [11].

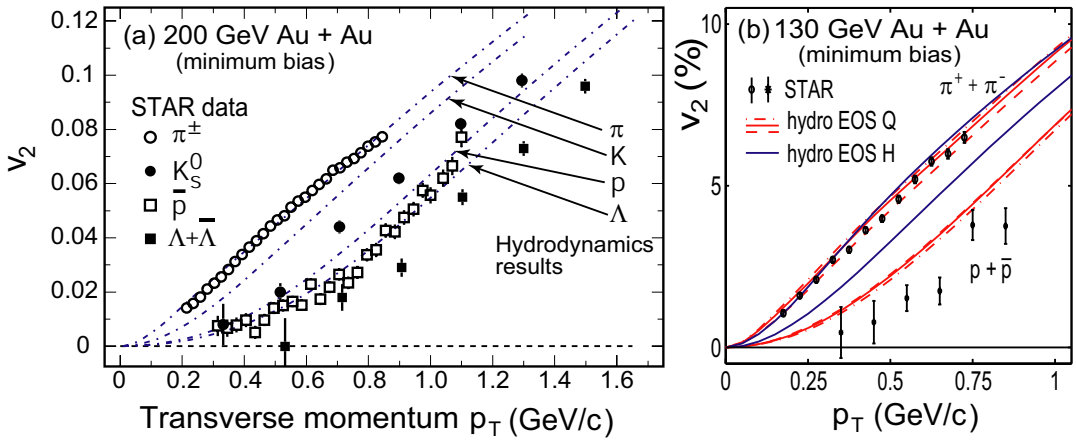

Figure 3. Left: Elliptic flow coefficient v_2 as function of p_t for different particle species [27]. Together with the experimental data results from a hydrodynamics calculation including a phase transition are shown [30]. Right: Experimental data for pions and protons at a lower RHIC energy [26]. Also shown are hydrodynamics calculations [30] with and without phase transition from QGP to hadronic phase. Figure from [7].

is well established for pp and e^+e^- collisions appears to be completely lifted. This leads to an enhancement in the yields of particularly multistrange hadrons in heavy ion collisions as compared to pp results. For the Omega baryon at SPS energy this enhancement is [13] a factor 17. How hadrons like the Ω can be equilibrated on the time scales of the nuclear collision has been a puzzle for several years and there is consensus that with two-body collisions and the known hadronic cross sections this is not possible [14,15,16]. A possible explanation has been presented recently [14]. In the direct vicinity of the phase transition the densities of particles are rising very rapidly due to the increase of degrees of freedom by more than a factor of 3 between a hadron gas and a QGP. At these high densities multi-hadron collisions become dominant and can drive even the Ω yield into equilibrium in a fraction of a fm/c. Conversely, already 5 MeV below the critical temperature the densities are so low that the system falls out of equilibrium and the yields cannot follow anymore a decreasing temperature. Therefore the authors of [14] conclude that the rapid equilibration is a direct consequence of the phase transition from QGP to hadronic matter and that, at least at high beam energies, the chemical equilibration temperature is a direct experimental measure of the critical temperature.

2.2 Elliptic Flow

Momentum distributions in three dimensions are analyzed with transverse coordinates relative to the reaction plane of the collision spanned by the impact parameter vector and the beam direction and a decomposition in terms of Fourrier coefficients is performed. Already at the Bevalac sizeable anisotropies were observed for heavy colliding nuclei. In particular, the quadrupole coefficient v_2 was found to be negative, explained by shadowing of the emitted particles by the target and projectile spectator remnants [17]. At AGS energies a sign change was observed [18] by E877, i.e. the momentum spectra were harder in the reaction plane than perpendicular to it. The interpretation used a prediction from hydrodynamics [19] that, for semiperipheral collisions, in the early phase of the collision the

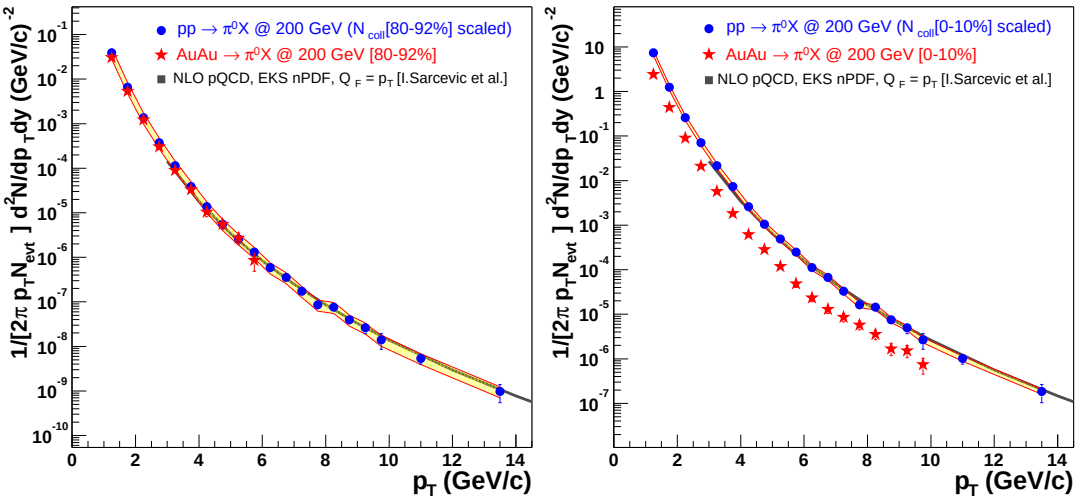

Figure 4. Neutral pion transverse momentum spectra measured by PHENIX in peripheral (left) and central (right) Au + Au collisions (stars) together with pp data from the same experiment scaled with the number of binary collisions (circles) [37,38]. Yellow band: Normalization uncertainties of the pp data. Black line: NLO pQCD calculation. Figure taken from [39].

pressure gradient was larger in this direction due to the excentricity of the nuclear overlap region[a]. From the hydrodynamic evolution it would follow, that this anisotropy in pressure gradient would evolve with time into an anisotropy in momentum space, driven by the initial condition and the equation of state of the expanding system. This was confirmed by a microscopic analysis within a transport model [21]. From this the name 'elliptic flow' originated for the quadrupole coefficient v_2.

At the higher SPS energy growing positive coefficients v_2 were found [22,23,24] and the sign change was traced to occur [25] at beam momenta per nucleon of about 4 GeV/c. At RHIC energies very large values of v_2 were observed [26,27,28,29], typically about 50 % above SPS top energy results.

This was studied differentially for different hadronic species and as function of p_t as shown for data from STAR in Figure 3. It is observed that for more massive hadrons the rise of v_2 starts at larger values of p_t. For the first time there was quantitative agreement with hydrodynamic calculations [30,31] in terms of p_t and hadronic species dependence, as also shown in Fig. 3. These hydrodynamic calculations also reproduce the overall features of the p_t spectra of differenct hadrons, although in details there are deviations stemming from the different treatment of the hadronic phase and freeze-out (see Fig. 20 in [8] and references there). It is common to all the hydrodynamics calculations that, in order to reproduce the data, a rapid initial equilibration on a time scale faster than 1 fm/c is required [30,31,32].

At p_t above 2-3 GeV/c, where hydrodynamics should no longer hold as a theoretical description, another type of scaling was discovered [33,7]: dividing both v_2 and p_t by the number of constituent quarks in a hadron all results match rather well even including multistrange baryons. It was realized that an old idea of quark coalescence [34] could be the underlying physics [35] and indeed calculations based on the assumption of coalescence of valence quarks during hadronization of a QGP reproduce this feature rather well [36].

[a] The use of hydrodynamics to describe the dynamics of a hadronic collision goes back to the 1950ies [20].

2.3 *High Momentum Suppression*

One of the highlights of the RHIC experimental program is the observation of a strong suppression in the production of hadrons at high transverse momentum when compared to pp collisions. Figure 4 shows the p_t spectrum of neutral pions in Au + Au collisions as compared to a measurement in pp in the same experiment and at the same energy [37,38]. The pp spectrum compares well with a calculation in NLO pQCD. In order to compare, the pp spectrum has been scaled with the number of binary nucleon-nucleon collisions in a Au + Au collisions at a given centrality. The number N_{coll} of binary collisions is given by the collision geometry - measured in the data with some resolution -, the well known nuclear density distribution, and the inelastic pp cross section. The collision centrality in Au + Au collisions is characterized by the fraction of the geometric cross section for which events have been selected, which is related to the impact parameter. The yellow bands in Fig. 4 reflect the systematic uncertainty in this scaling. One can observe that for peripheral collisions pp and Au + Au collisions agree very well, while in central collisions the Au + Au spectrum is significantly suppressed.

This is better visualized by building the ratio R_{AA} between the Au + Au p_t spectrum and the pp spectrum scaled with N_{coll} as shown in Figure 5. All four RHIC experiments observe a suppression by about a factor of five for p_t larger than 4 GeV/c. Since not all experiments measure neutral pions, the ratio is shown here for charged hadrons, but at large p_t the data for all hadron species merge. At low p_t the ratio R_{AA} is expected to be below one because there, due to the dominance of soft processes, the appropriate scaling is with the number of participants, i.e. nucleons in the nuclear overlap region. It is expected that this ratio should rise as hard scattering becomes dominant and, in fact,

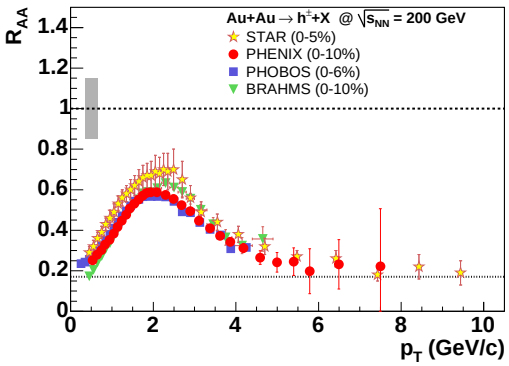

Figure 5. Ratio R_{AA} of the p_t spectrum for central Au + Au collisions normalized to the pp spectrum scaled with the number of binary collisions for charged particles from all four RHIC experiments. Figure from [40].

due to the well known Cronin enhancement, in the region of 2-6 GeV/c values above one are expected. Contrary to this expectation the data show a suppression.

The suppression is not unexpected. It was predicted that in a medium with high parton density the radiative energy loss of a quark or gluon should be strongly enhanced [41,42], leading to a very effective thermalization of jets in a hot color charged medium. Calculations employing a large initial gluon rapidity density of about 1100 can account [43] for the data at top RHIC energy. The beam energy dependence of the R_{AA} ratio was presented recently by d'Enterria [44] and it appears that the suppression evolves in a very smooth way from top SPS energy onwards. The $R_{AA}(p_t = 4\mathrm{GeV/c})$ values are shown in Figure 6 for the top SPS energy and three RHIC energies. Already the values of about 1.0 measured at the SPS represent a slight suppression as compared to the normal Cronin enhancement [44]. Going from $\sqrt{s_{nn}} = 17.3$ to 62.4 to 200 GeV the gluon rapidity density needed to reproduce the data grows [43] from 400 to 650 to 1100. An alternative formulation of this in medium suppression is by increasing and large opacities of the medium traversed [45].

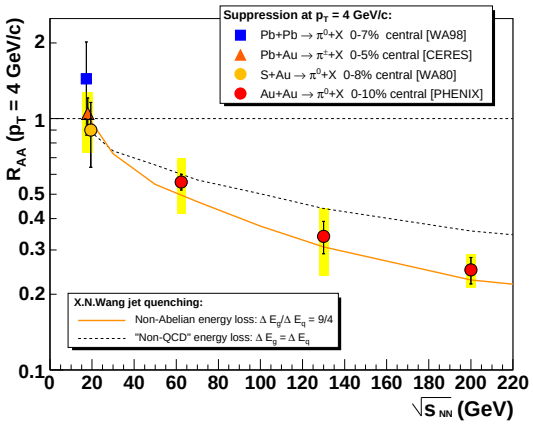

Figure 6. Suppression factor R_{AA} for pions as function of beam energy at a fixed p_t value of 4 GeV/c. The yellow line shows a calculation [45] including parton energy loss in a medium with high parton density. Figure from [44].

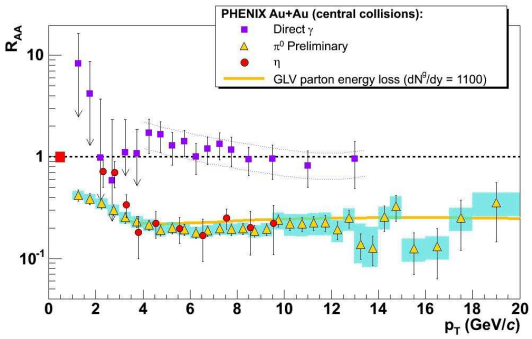

Figure 7. Preliminary PHENIX results for the suppression factor R_{AA} out to high p_t for π^0 and η mesons together with a calculation based on a high gluon rapidity density [43]. Also shown are the results for direct photons. Figure from [53].

The proof that this is really a final state effect probing the properties of the medium traversed by the parton is given by the observation that in d + Au collisions in the same experiments no suppression is seen, but rather the expected Cronin enhancement [46,47,48,49].

Direct photons were measured by PHENIX in pp and Au + Au collisions at top RHIC energy [50,51]. The pp spectra are rather close to a NLO pQCD calculation [52]. The Au + Au photon spectra are within errors consistent with the scaled pp result and hence the expectation from NLO pQCD. For all centralities they do not show any significant suppression. This is shown in Figure 7 where also the most recent neutral pion results from run4 [53] extending out to p_t = 20 GeV/c are displayed. It is remarkable that the suppression of the pion p_t spectrum remains practically constant over a large range in p_t from 4 to 20 GeV/c, close to the predicted behavior for a medium with initial gluon rapidity density of 1100 (see Fig. 7).

The high initial gluon densities correspond to an initial temperature of about twice the critical temperature and to initial energy densities ϵ_0 = 14 - 20 GeV/fm^3 well in line with the initial conditions needed for the hydrodynamics calculations to describe spectra and elliptic flow (see previous section) and bracketed by the estimates based on the Bjorken formula and transverse energy production.

The observed high p_t suppression pattern is different for different hadronic species [5,8,7]. In particular, a pattern appears where at intermediate values of p_t of 2-6 GeV the suppression of baryons is significantly weaker than that of mesons. The proton/pion or also the Λ/K^0_s ratios peak at values 1.5-1.6 for p_t = 3-4 GeV/c, close to the ratio 3/2 expected in quark coalescence models.

Parton thermalization is displayed in a very clean way be recent results of the STAR collaboration [54]. Evaluating the mean transverse momentum in a cone opposite to a high p_t trigger particle as a funtion of centrality, a gradual decrease for more central Au + Au collisions is observed and in the most central collisions a value very close to the inclusive mean p_t is reached (see Figure 8).

In azimuthal correlations of two high p_t particles it was seen that the away-side peak disappears in central Au + Au collisions

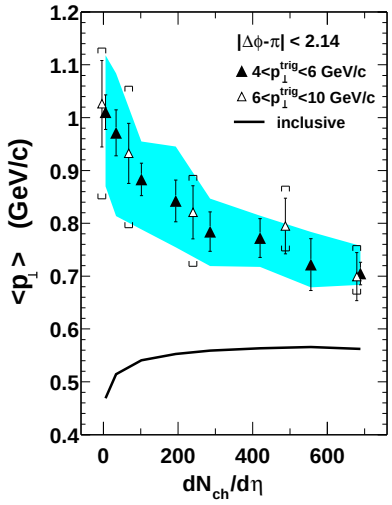

Figure 8. Mean transverse momentum in a cone of an opening angle of one radian opposite to a leading particle as a function of the collision centrality; distributions are for two ranges of leading particle transverse momentum as well as for the inclusive particle distribution. Data and figure from STAR [54].

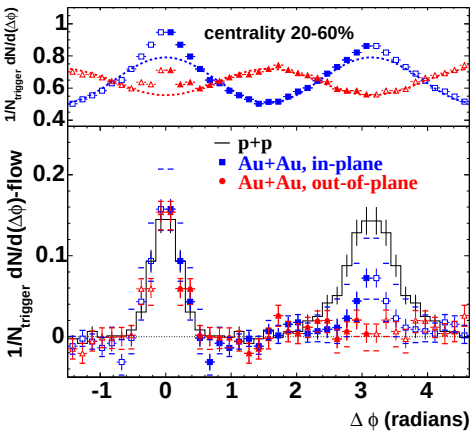

Figure 9. Azimuthal angle correlation between a high p_t trigger particle (4-6 GeV/c) with all particles in the window p_t = 2-4 GeV/c for intermediate centrality Au + Au collisions. The distribution is shown for both particles in a ± 45 degree window around the reaction plane orientation (in-plane) or a same window perpendicular to it (out-of-plane). Figure from [56].

for a choice of trigger p_t of 4-6 GeV and p_t of the correlated particle of 2-4 GeV/c [55]. In pp, d + Au and peripheral Au + Au collisions a clear peak opposite to the trigger particle is observed in the same type of correlation, also measured by STAR [55,48]. Recently, it was shown that the effect is very strong in case the away-side jet is emitted out of the reaction plane and much weaker for emission in the reaction plane [56] as displayed in Figure 9. This supports the strong correlation of the suppression with the length of matter traversed by the parton.

When lowering the p_t cut on the correlated hadron, a very broad structure appears on the side opposite to the trigger particle. This was shown by STAR [54] for a cut on the correlated hadron of p_t = 0.15 - 4 GeV/c. This calls to mind a similar observation at SPS energy by CERES [57] where for a condition $p_t \geq 1.2$ GeV/c for both particles also very strong broadening of the away-side structure with increasing collision centrality in Pb + Au collisions was observed. Recent data [58] from PHENIX display a tantalizing feature as shown in Figure 10: For a trigger particle p_t of 4-6 GeV/c and a correlated particle p_t of 1.0 - 2.5 GeV/c the away-side peak seen in peripheral Au + Au collisions develops actually into a hole at $\Delta\phi = \pi$ for more central collisions while a very broad peak appears with a maximum at $\Delta\phi = \pi - 1$ as can be seen in Fig. 10. A suggestion has been made that this could be the Mach cone due to the sonic boom of the quenched jet. A parton traversing a quark-gluon plasma with velocity larger than the velocity of sound in the QGP ($\sqrt{1/3}$ for an ideal gas) would radiate only up to a cone angle of about 1 rad [59,60]. If this could be established it would have far reaching consequences since it would be an observable linked directly to the speed of sounds of the quark-gluon plasma and thereby its equation of state. It remains an experimental challenge to establish an actual cone topology in two dimensions.

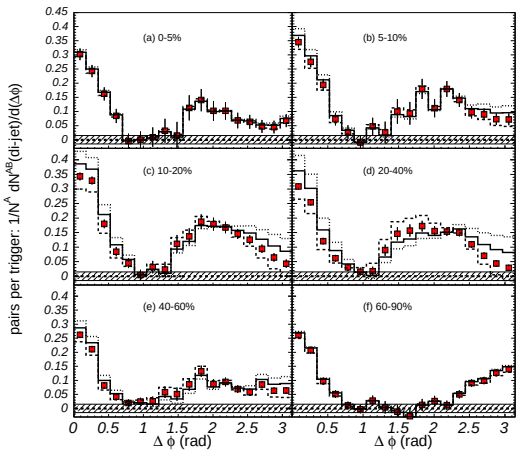

Figure 10. Azimuthal correlations of a leading particle of p_t = 4-6 GeV/c and any particle with p_t = 1-2.5 GeV/c for different centralities of a Au + Au collision. Data and figure from PHENIX [58].

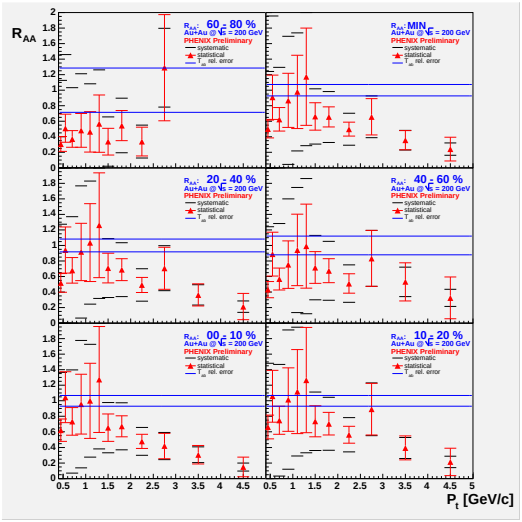

Figure 11. R_{AA} suppression factor for electrons dominantly from open charm and open beauty decay for Au + Au collisions at top RHIC energy for different collision centrality (see text) measured by PHENIX. Figure from [64].

2.4 Charm Quarks and Quarkonia

Open charm has been measured indirectly from the inclusive electron p_t spectra after subtracting known contributions from photon conversions and light hadron decays by PHENIX [61]. The spectrum remaining after subtraction is dominated [b] by open charm and beauty contributions. Recently results for an elliptic flow analysis were shown [62] of the electrons dominantly from open charm decays. There is a significant nonzero value in the p_t range 0.4 - 1.6 GeV/c. This is confirmed by preliminary STAR data [63] that extend the overall transverse momentum coverage by adding the range p_t = 1.5 - 3.0 GeV/c. Together, the data paint a consistent picture that indeed the electrons from open charm decay exhibit elliptic flow, i.e. follow the collective motion of the light quarks. This would imply that the charm quark thermalizes to a significant degree. Note that this is a necesarry prerequisite for any formation of charmed hadrons by statistical hadronization (see below).

In that case also jet quenching should be observed for charmed hadrons. Indeed, in still preliminary data it was shown recently that electron spectra, after the subtraction of contributions from conversion and light hadron decays, show high p_t suppression for central Au + Au collisions [64]. The R_{AA} factor drops practically as low as for pions at p_t of 4 GeV/c, i.e. to values of about 0.2. In a recent publication [65] the suppression for electrons from D meson decay was studied for different transport coefficients. The preliminary RHIC data would be consistent with a calculation using a transport coefficient of 14 GeV^2/fm (see Fig. 2 of [65]), at the upper end of the range needed to reproduce R_{AA} for pions. This is very surprizing, in particular also in view of the fact, that at p_t of about 4 GeV/c also the contribution of b-quarks to the electron spectrum should become sizeable.

At top SPS energy, for central Pb + Pb

[b] A possible contribution to the electron spectrum from the Drell-Yan process cannot be ruled out at present, though.

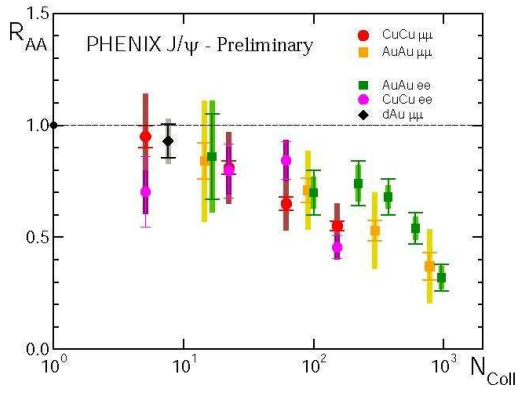

Figure 12. J/ψ yield in Au + Au and Cu + Cu collisions at top RHIC energy normalized to the measured result for pp collisions, scaled with the number of inelastic collisions. Results are shown for decays into electron and muon pairs at mid- and forward rapidities, respectively. Figure from [53].

collisions a significant suppression of J/ψ production was observed in the NA50 experiment [66,67]. This suppression is compared to the socalled 'normal' nuclear absorption seen also in pA collisions. From analysis of all pA data, a cross section for normal nuclear absorption of 4.1±0.4 mb was extracted [67]. To this normal nuclear absorption all results from heavy ion collisions can be compared. It turns out that S + U data as well as data from peripheral Pb + Pb collisions agree with this normal nuclear absorption curve. For transverse energies above 40 GeV or a length of nuclear matter seen by the J/ψ of L $\geq$ 7 fm the points from Pb + Pb collisions fall increasingly below this normal nuclear absorption curve. Theoretically, the suppression can be explained by disappearance of the J/ψ (or possibly only the charmonia states that feed it) in a hot colored medium or by interaction with comovers (chiefly pions), albeit with a very large density of more than 1/fm^3, i.e. a value not deemed achievable for a hadron gas.

The first results for J/ψ production in central Au + Au collisions at RHIC energy came very recently from PHENIX [53] (run4); they are displayed in Figure 12. As compared to pp as well as d + Au collisions there is a significant suppression. The suppression is, however, rather similar to the one observed at SPS. This is in contrast to some predictions [68] that in central Pb + Pb collisions at RHIC only J/ψ mesons from the corona should survice, i.e. order of 5 % of the normal unsuppressed yield. The actually observed yield by far exceeds this expectation. This could be seen as indication, that at RHIC the energy density in the QGP is not yet high enough to dissolve the J/ψ but rather only enough to dissolve higher c$\bar{\text{c}}$ states. Recent results from high temperature lattice QCD indicate that the J/ψ bound state may only disappear [69] in the vicinity of T = 2 T$_c$.

A maybe more interesting alternative has been proposed [70]: Even if the initially formed c$\bar{\text{c}}$ pairs are completely dissociated in the hot QGP, at hadronization charmed hadrons may form in a statistical fashion by the same mechanism described above for hadrons involving up, down, and strange valence quarks. This includes also the formation of charmonia and it was pointed out in [70] that the formation probability of J/ψ mesons would grow quadratically with the c$\bar{\text{c}}$ rapidity density. Such increased reformation of J/ψ by statistical hadronization could possibly account for a suppression apparently not much stronger than at SPS.

Figure 13 shows the prediction of [71] together with the recent and still preliminary RHIC data for J/$\psi \rightarrow e^+e^-$. Currently the main uncertainty in this consideration is the overall charm production yield, which enters quadratically. A calculation is shown using a cross section per unit rapidity of 80 μb (400 μb integrated) as expected from NLO pQCD [68]. The overall charm production cross section at RHIC energy has so far been measured indirectly by PHENIX [61] for $\sqrt{s}$ = 130 and 200 GeV from the inclusive elec-

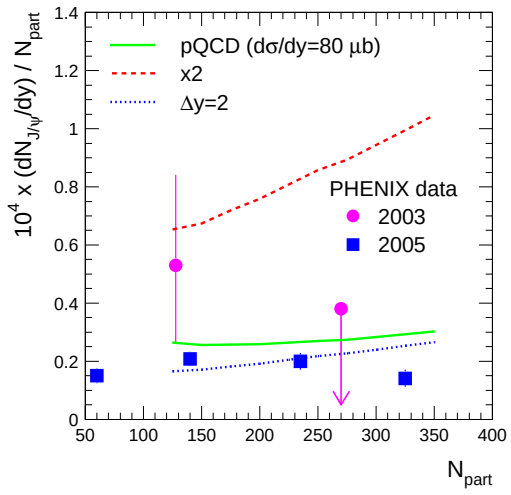

Figure 13. J/ψ yield per participating nucleon for Au + Au collisions at top RHIC energy compared to the yield expected from statistical recombination. Data from [53], statistical hadronization prediction from [71]. For statistical hadronization a standard interval of Δ y = 1 is used. Calculations are shown for a $c\bar{c}$ cross section per unit rapidity of 80 μb, of 160 μb. Also shown: a calculation for 80 μb and Δ y = 2.0.

tron spectra in the way described above for Au + Au collisions and, at full RHIC energy, also for d + Au and pp collisions [72]. It is found that the integrated charm cross section, when scaled with the number of binary collisions, agrees for all three collision systems. The value is about 50% above the NLO pQCD calculation [68] but agrees within errors. On the other hand, in STAR, D mesons have been reconstructed via their hadronic decay to Kπ in d + Au collisions and a charm cross section per nucleon nucleon collision has been extracted [73]. It is twice as large as the PHENIX value by nearly two standard deviations. The experimental situation concerning open charm production needs to be improved before the J/ψ puzzle can be better addressed. Only measurements at LHC will unambiguously clarify the role of statistical hadronisation of charm, since with this mechanism a significant J/ψ enhancement in Pb + Pb collisions at LHC was predicted [71] instead of suppression. Such an enhancement would be an unambiguous signal of deconfinement.

3 Summary and Outlook

Hadron yields are found to be in chemical equilibrium. For top SPS energy and up this can be achieved by multi-particle collisions in the direct vicinity of T_c and hence the observed chemical equilibration temperature is an experimental measure of the critical temperature for the phase transition.

At RHIC energies, spectra and azimuthal correlations are quantitatively described by hydrodynamics. This requires rapid local thermalization and high initial energy densities more than tenfold above the calculated critical energy density for the phase transition between hadronic matter and QGP.

High p_t hadrons are suppressed in central Au + Au collisions and this is a medium effect. Jet quenching in a hot color charged medium was predicted, modelling of the data with high parton density is successful. There are some indications of valence quark coalescence in hadronic observables.

The observations that lead to the CERN press release are confirmed by the RHIC experiments. Beyond this additional features are observed that start to probe the properties of the new state of matter. Much progress in this direction is expected from the high luminosity RHIC data just starting to appear and, from 2007, from the LHC heavy ion program.

Acknowledgements

I thank Peter Braun-Munzinger for numerous enlightening discussion.

References

1. D.J. Gross, F. Wilczek, *Phys. Rev. Lett.* **30** 1343 (1973); H.D. Politzer, *Phys. Rev. Lett.* **30** 1346 (1973).

2. J.C. Collins, M.J. Perry, *Phys. Rev. Lett.* **34** 1353 (1975); N. Cabibbo, G. Parisi, *Phys. Lett. B* **59** 67 (1975).
3. F. Karsch, *Nucl. Phys. A* **698** 199c (2002), hep-ph/0103314.
4. CERN press release Feb. 10, 2000; U. Heinz and M. Jacob, nucl-th/0002042.
5. I. Arsene et al., BRAHMS Collaboration, *Nucl. Phys. A* **757** 1 (2005), nucl-ex/0410020.
6. B.B. Back et al., PHOBOS Collaboration, *Nucl. Phys. A* **757** 28 (2005), nucl-ex/0410022.
7. J. Adams et al., STAR Collaboration, *Nucl. Phys. A* **757** 102 (2005), nucl-ex/0501009.
8. K. Adcox et al., PHENIX Collaboration, *Nucl. Phys. A* **757** 184 (2005), nucl-ex/0410003.
9. P. Braun-Munzinger, K. Redlich, and J. Stachel, in Quark-Gluon Plasma 3, eds. R.C. Hwa and X.N. Wang, (World Scientific, Singapore, 2004), 491.
10. P. Braun-Munzinger, D. Magestro, K. Redlich, and J. Stachel, *Phys. Lett. B* **518** 41 (2001).
11. updated version of Figure in P. Braun-Munzinger, J. Stachel, *J. Phys. G* **28** 1971 (2002), taken from A. Andronic, P. Braun-Munzinger, J. Stachel, to be published.
12. Z. Fodor, S.D. Katz, *J. High Ener. Phys.* **404** 50 (2004), hep-lat/0402006.
13. E. Andersen et al., WA97 Collaboration, Phys. Lett. B **449** 401 (1999).
14. P. Braun-Munzinger, J. Stachel, and C. Wetterich, *Phys. Lett. B* **596** 61 (2004).
15. C. Greiner, *AIP Conf.Proc.* **644** 337 (2003).
16. P. Huovinen, J.I. Kapusta, *Phys. Rev. C* **69** 014902 (2004).
17. H. Gutbrod et al., *Phys. Rev. C* **42** 640 (1990).
18. J. Barrette et al., E877 Collaboration, *Phys. Rev. C* **55** 1420 (1997).
19. H. Stöcker, W. Greiner, *Phys. Rept.* **137** 277 (1986).
20. L.D. Landau, *Izv. Akad. Nauk. Ser. Fiz.* **17** 51 (1953).
21. H. Sorge, *Phys. Lett. B* **402** 251 (1997).
22. H. Appelshäuser for the NA45 Collaboration, Proc. QM2001; G. Agakichiev et al., NA45 Collaboration, *Phys. Rev. Lett.* **92** (2004) 032301.
23. C. Alt et al., NA49 Collaboration, *Phys. Rev. C* **68** 034903 (2003).
24. M.M. Aggarwal et al., WA98 Collaboration, *Eur. Phys. J. C* **41** 287 (2005).
25. P. Chung et al., E895 Collaboration, *Phys. Rev. C* **66** 021901 (2002).
26. C. Adler et al., STAR Collaboration, *Phys. Rev. Lett.* **87** 182301 (2001).
27. J. Adams et al., STAR Collaboration, *Phys. Rev. Lett.* **92** 052302 (2004).
28. S.S. Adler et al., PHENIX Collaboration, *Phys. Rev. Lett.* **91** 182301 (2003).
29. B.B. Back et al., PHOBOS Collaboration, *Phys. Rev. Lett.* **89** 222301 (2002).
30. P. Huovinen, P.F. Kolb, U.W. Heinz, P.V. Ruuskanen, and S.A. Voloshin, *Phys. Lett. B* **503** 58 (2001); P. Huovinen, private communication.
31. D. Teaney, J. Lauret, and E.V. Shuryak, *Phys. Rev. Lett.* **86** 4783 (2001) and nucl-th/0110037.
32. P.F. Kolb, U. Heinz, in Quark-Gluon Plasma 3, eds. R.C. Hwa and X.N. Wang, (World Scientific, Singapore, 2004) 634.
33. X. Dong, S. Esumi, P. Sorensen, and N. Xu, *Phys. Lett. B* **597** 328 (2004).
34. K.P. Das, R.C. Hwa, *Phys. Lett. B* **68** 459 (1977); Erratum-ibid.**73** 503 (1978).
35. S.A. Voloshin, *Nucl. Phys. A* **715** 379c (2003).
36. R.J. Fries, B. Müller, C. Nonaka, S.A. Bass, *Phys. Rev. Lett.* **90** 202303 (2003).
37. S.S. Adler et al., PHENIX Collaboration, *Phys. Rev. Lett.* **91** 072301

(2003).
38. S.S. Adler et al., PHENIX Collaboration, *Phys. Rev. Lett.* **91** 241803 (2003).
39. D. d'Enterria for the PHENIX Collaboration, inv. talk at Nato Adv. Study Inst., Kemer, Turkey, 2003, nucl-ex/0401001.
40. D. d'Enterria, Proc. Renc. de Moriond 2004, nucl-ex/0406012.
41. X.N. Wang and M. Gyulassy, *Phys. Rev. Lett.* **68** 1480 (1992).
42. H. Baier, Y.L. Dokshitzer, A.H. Mueller, S. Peigne, and D. Schiff, *Nucl. Phys. B* **483** 291 (1997) and **B84** 265 (1997).
43. I. Vitev, Proc. ICPAQGP, Kolkata 2005, *J. Phys. G* in print, hep-ph/0503221.
44. D. d'Enterria, Proc. "Hard Probes 2004", *Eur. Phys. J. C*, in print, nucl-ex/0504001.
45. Q. Wang and X.N. Wang, *Phys. Rev. C* **71** 014903 (2005).
46. B.B. Back et al., PHOBOS Collaboration, *PRL* **91** 072302 (2003).
47. S.S. Adler et al., PHENIX Collaboration, *PRL* **91** 072303 (2003).
48. J. Adams et al., STAR Collaboration, *PRL* **91** 072304 (2003).
49. I. Arsene et al., BRAHMS Collaboration, *PRL* **91** 072305 (2003).
50. S.S. Adler et al., PHENIX collaboration, *Phys. Rev. D* **71** 071102R (2005).
51. S.S. Adler et al., PHENIX collaboration, *Phys. Rev. Lett.* **94** 232301 (2005).
52. L.E. Gordon and W. Vogelsang, *Phys. Rev. D* **48** 3136 (1993).
53. Y. Akiba for the PHENIX collaboration, Proc. Quark Matter 2005 Conference, *Nucl. Phys. A* , in print, nucl-ex/0510008.
54. J. Adams et al., STAR Collaboration, nucl-ex/0501016.
55. C. Adler et al., STAR Collaboration, *Phys. Rev. Lett.* **90** 082302 (2003).
56. J. Adams et al., STAR Collaboration, *Phys. Rev. Lett.* **93** 252301 (2004).
57. D. Adamova et al., CERES Collaboration, *Phys. Rev. Lett.* **92** 032301 (2004).
58. S.S. Adler et al., PHENIX Collaboration, nucl-ex/0507004.
59. H. Stöcker, *Nucl. Phys. A* **750** 121 (2005).
60. J. Casalderrey-Solana, E. Shuryak, and D. Teaney, hep-ph/0411315.
61. K. Adcox et al., PHENIX Collaboration, *Phys. Rev. Lett.* **88** 192303 (2002); S.S. Adler et al., PHENIX Collaboration, *Phys. Rev. Lett.* **94** 082301 (2004).
62. S.S. Adler et al., PHENIX Collaboration, nucl-ex/0503003.
63. M.A.C. Lamont for the STAR Collaboration, Proc. ICPAQGP Kolkata 2005, *J. Phys. G* in print.
64. B. Jacak for the PHENIX collaboration, Proc. ICPAQGP Kolkata 2005, *J. Phys. G* in print, nucl-ex/0508036.
65. N. Armesto, A. Dainese, C.A. Salgado, U. Wiedemann, *Phys. Rev. D* **71** 054027 (2005).
66. M.C. Abreu et al., NA50 Collaboration, *Phys. Lett. B* **521** 195 (2001).
67. B. Alessandro et al., NA50 Collaboration, *Eur. Phys. J. C* **39** 335 (2005).
68. R. Vogt, *Int. J. Mod. Phys. E* **12** 21 (2003); and hep-ph/0203151.
69. F. Karsch., Proc. Int. Conf. Hard and Electromagnetic Probes, Ericeira, Portugal 2004, hep-lat/0502014.
70. P. Braun-Munzinger, J. Stachel, *Phys. Lett. B* **490** 196 (2000).
71. A. Andronic, P. Braun-Munzinger, K. Redlich, J. Stachel, *Phys. Lett. B* **571** 36 (2003).
72. K. Adcox et al., PHENIX Collaboration, *J. Phys. G* **30** S1189 (2004).
73. J. Adams et al., STAR Collaboration, *Phys. Rev. Lett.* **94** 062301 (2005).